Hindawi
International Journal of Aerospace Engineering
Volume 2022, Article ID 6495746, 19 pages
https://doi.org/10.1155/2022/6495746

Research Article

A New United Proportional Navigation Guidance for Impact Angle Constraint without Measurement Distance between Vehicle and Target

Hao Yang, Hangjin Wu, Xibin Bai, and Shifeng Zhang

College of Aerospace Science and Engineering, National University of Defense Technology, Changsha 410073, China

Correspondence should be addressed to Hao Yang; yanghao16@nudt.edu.cn

Received 19 May 2022; Revised 20 October 2022; Accepted 8 November 2022; Published 30 November 2022

Academic Editor: Shaoming He

This paper proposed a united proportional navigation guidance (UPNG) method to alleviate the guidance command saltation with an impact angle constraint under the condition of no real-time distance between the vehicle and the target (line-of-sight (LOS) distance). Firstly, based on the biased proportional navigation guidance (BPNG), a smooth-biased proportional navigation guidance (SBPNG) method was proposed, whose bias term was designed as a trigonometric function. In SBPNG method, due to the continuous smooth change of the bias term, the guidance command would not saltus anymore, and the impact angle was controlled by the bias integral component. Secondly, biased on SBPNG method, the united proportional navigation guidance (UPNG) method combining SBPNG and variable coefficient proportional navigation guidance (VCPNG) was established. In UPNG method, because there was no LOS distance, the guidance coefficient was designed as a function of the difference between the expected impact angle and the estimated impact angle, so the closed-loop control of impact angle was realized. Finally, a lot of simulation experiments on different guidance laws were carried out without real-time LOS distance. The results verify that the UPNG method proposed in this paper solves the problem of guidance command saltation effectively and has better robustness in impact angle control.

1. Introduction

Guidance laws are divided into classical guidance and modern guidance laws which play an essential role in the development of precision weapons. Classical guidance laws are represented by the tracking method [1], the parallel approach method [2], proportional navigation guidance method, etc. [3–5]. Both the tracking method and parallel approach method can be classified into PNG methods [6]. As a classical guidance laws, PNG method has a wide application in engineering practice [7], owing to its simple structure, easy implementation, less information required, straight trajectory, high guidance accuracy, applicability for maneuvering targets, and other desirable qualities [8]. However, pure proportional navigation guidance (PPNG) cannot satisfy impact angle constraints. In order to solve this problem, two types of methods, BPNG and VCPNG, are proposed to realize impact angle constraints.

Kim et al. pioneered the application of the optimal BPNG to the impact angle constraint, with the bias term as a function of LOS distance [9]. Later, some scholars designed the bias term as a function of the time-to-go [10, 11]. In [12], BPNG was combined with convex optimization to solve the problem of rocket vertical soft landing with impact angle constraints. Lee et al. considered the field-of-view angle constraints and designed a guidance law satisfying impact angle constraints based on the tracking method and PNG method [13]. Zhang et al. adopted the switching control logic and added a bias switch based on the BPNG method with impact angle constraints ensuring that the target lies within the seeker's field-of-view [14]. Kim et al. proposed a guidance law which can control the impact time by adjusting the coefficient under restricted conditions of field-of-view angle. And the impact angle constraint is satisfied through the sliding mode control method [15]. Real-time LOS distance or time-to-go for

the methods mentioned above is necessary. The time-to-go is also obtained by real-time LOS distance. But, for most precision-guided munitions (such as those based on infrared and laser guidance), their seekers cannot provide information about LOS distance. Studies have demonstrated that once time-to-go estimation is inaccurate, the ability of such guidance laws for impact angle constraint will fall sharply [16, 17]. Therefore, there is an urgent need for a guidance law with impact angle constraints which do not require the LOS distance or time-to-go.

Erer and Ozgoren and Erer and Merttopçuoglu proposed a BPNG law without information about time-to-go or LOS distance [18, 19]. By delving into the relationship between the bias integral component and the impact angle, Erer and Merttopçuoglu and Sun et al. controlled the bias integral component, thereby achieving impact angle control [20, 21]. Ratnoo proposed two-stage VCPNG and verified the effective control of the impact angle through numerous simulations [22]. Tekin and Erer proposed a two-stage PNG which could realize field-of-view angle constraint, overload constraint, and impact angle constraint, as the coefficient of PNG was designed as a function of the seeker's maximum field-of-view angle, maximum overload, and expected impact angle [23]. Ratnoo and Ghose also extended the two-stage BPNG method to conduct omnidirectional attack on moving targets [24]. Wang studied the relationship between the bias integral component and the impact angle and achieved precise control of the impact angle by strictly controlling the duration of the bias term [25]. Ratnoo studied the ballistic properties under different scale coefficients and realized precise control of the impact angle by adjusting the coefficients in different stages and the switching time of guidance parameters [26]. Most of the aforementioned methods are two-stage guidance methods that involve guidance command saltation before and after first stage. And they almost all belong to open-loop control in terms of impact angle constraints. Therefore, it is a problem worth studying to realize the closed-loop control of the impact angle without real-time LOS distance while ensuring that the guidance command do not saltate.

To solve the problem of overload command saltation, Zhou et al. suggested a nonlinear extended state observer to estimate the unmeasurable disturbance of the system and avoided guidance command saltation through the compensating system [27]. Amit et al. proposed to add a transition section between the first stage and the second stage to smoothen the guidance command [28]. Although these two methods effectively solve the problem of guidance command saltation, the impact angle constraint is unsatisfied. Considering the limitations of the seeker's field-of-view, Lu and David proposed a similar BPNG composed of PNG and impact angle error feedback, which makes the guidance command continuous by removing the guidance switch [29]. To avoid command saltation caused by the sudden intervention of the bias term, the proportion of the bias term was adequately adjusted through multiplying the bias term by a time-varying constraint coefficient [24]. However, both methods have coefficients that are a function of the time-to-go. Therefore, the ways in which to smoothen the guidance command without LOS distance and the time-to-go, considering impact angle constraints, merit further academic scrutiny. Focusing on the above problems, the main contributions of this paper are as follows:

(1) Under the condition of no LOS distance and time-to-go, the SBPNG method with continuous and smooth guidance command is presented. By adopting the smoothing process in the form of a trigonometric function, this method effectively avoids guidance command saltation when guidance phases are switched

(2) Based on the SBPNG method and combined with the VCPNG method, UPNG method is proposed, in which the closed-loop control of the impact angle without LOS distance and the time-to-go is successfully achieved

(3) Based on the parameters of an experimental aircraft and considering various uncertain disturbances, numerous simulations are conducted on the proposed method and traditional methods. The effectiveness of the proposed method is verified through comparative analysis

The remainder of the paper is organized as follows. In Section 2, the PNG method with impact angle constraint is introduced, and the problem formulation and motivation are provided. The smoothing method SBPNG is introduced in Section 3. In Section 4, the method of UPNG is introduced. In Section 5, a large number of simulation results are given. Finally, the conclusion is provided in Section 6.

2. Problem Statement

In this section, an analysis is given on the basic principle of the variable coefficient PNG (VCPNG) method and the biased PNG (BPNG) method satisfying the impact angle constraints. The motivation of the smooth processing and development of the united PNG (UPNG) method are further derived.

2.1. Homing Guidance. The horizontal line within the attack plane is selected as the reference line. Polar coordinates are used to describe the relative movement of the vehicle and target. The geometric relationship and variable definition are shown in Figure 1. The angles are positive when rotated counterclockwise.

According to the principle of PNG, the relative motion model can be constructed as follows [26]:

$$\dot{R} = -V\cos\eta, \tag{1}$$

$$\dot{q} = \frac{-V\sin\eta}{R}, \tag{2}$$

$$\eta = \theta - q, \tag{3}$$

$$\dot{\theta} = N\dot{q}, \tag{4}$$

$$\dot{\eta} = -\frac{(N-1)V\sin\eta}{R}. \tag{5}$$

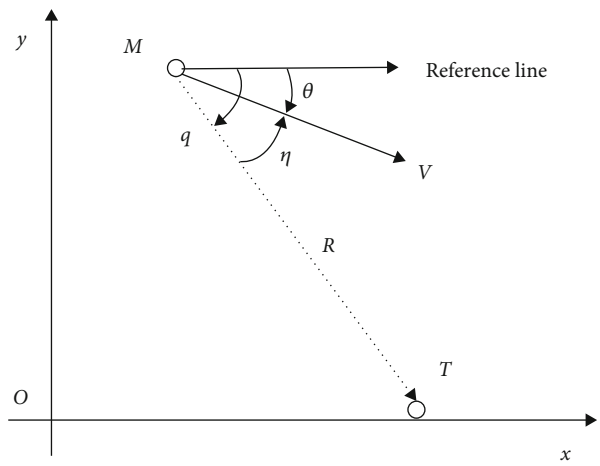

Figure 1: Guidance geometry.

So the relationship between R and η can be obtained:

$$\frac{d\eta}{dR} = \frac{N-1}{R}\tan\eta, \tag{6}$$

$$R = c|\sin\eta|^{1/N-1}, \tag{7}$$

where c is an integration constant. Consider the case of $0 < \eta(0) < \pi$ for the moment. Substituting (7) into (5) gives

$$\dot{\eta} = \frac{(1-N)V}{c}\sin\eta^{N-2/N-1}. \tag{8}$$

As the condition $\eta \in (0, \pi)$ is met when the vehicle attacks the ground target, the following conclusions can be drawn:

(1) If $N < 1$ and $\dot{\eta} > 0 \dot{q} < 0$, the look-ahead angle η will increase with time, while the LOS angle q will decrease with time

(2) If $N = 1$ and $\dot{\eta} > 0$, the look-ahead angle η will not vary with time. However, according to (2), the LOS angle q will decrease with the LOS distance

(3) If $N > 1$ and $\dot{\eta} < 0$, the look-ahead angle η will decrease with time, and conclusion can be drawn that $r \underset{\eta \longrightarrow 0}{\longrightarrow} 0$ by combining (6)

(4) If $N > 2$, there is $\dot{\eta} \longrightarrow 0, \dot{q} \longrightarrow 0, \dot{\theta} \longrightarrow 0$ as $\eta \longrightarrow 0$, which means that the vehicle will hit the target at a constant flight path angle as long as N is a certain value

The effective proportional coefficient N_e is defined as

$$N_e = \frac{\dot{\theta}}{\dot{q}}. \tag{9}$$

According to conclusion 4, in order to keep the terminal overload from diverging, N_e must be greater than 2 so that the precision guidance can be realized. So, the trajectory with the effective proportional coefficient N_e greater than 2 is defined as the convergence trajectory here.

Considering the terminal constraint of the vehicle hitting the target, that is, θ_f should be equal to the terminal LOS angle q_f. The terminal flight path angle θ_f can be obtained as follows by integrating (4).

$$\theta_f = q_0 - \frac{\eta_0}{N-1}. \tag{10}$$

The expected impact angle is usually denoted as $\Gamma = -\theta_f$. According to (10), the impact angle can be increased by increasing the look-ahead angle η_0 or decreasing the LOS angle q_0. All the above analyses are based on PPNG, which cannot control the impact angle. However, large impact angle constraints are often proposed in practice, such as vertical strike missions. So, the PNG with impact angle constraint is proposed.

2.2. Impact Angle Control Guidance Law. There are two ways to realize the impact angle constraint based on PNG, namely, biased PNG (BPNG) and variable coefficient PNG (VCPNG).

In BPNG, a bias term was added to PPNG to meet the impact angle constraint. So, the BPNG can be written as [25]

$$\dot{\theta} = N\dot{q} + b, \tag{11}$$

where b is bias term. The following equation is obtained by integrating (11).

$$\theta_f - \theta_0 = N\left(q_f - q_0\right) + B, \tag{12}$$

where $B = \int_0^t b dt$ represents the bias integral component. Under the hit condition $\theta_f = q_f$, the relationship between the expected impact angle and the required bias integral component can be described as follows.

$$B_N = (N-1)\Gamma + Nq_0 - \theta_0. \tag{13}$$

In the process of application, the size of the bias needs to be controlled to ensure that (13) is satisfied when the vehicle hits the target; thus, the impact angle can be achieved.

The VCPNG method satisfies the impact angle constraint by changing the proportional coefficient N. According to the conclusion of the previous analysis, the look-ahead angle η increases with time when $N \leq 1$, and the LOS angle decreases with time when $N \leq 1$, which can achieve a large impact angle. Therefore, $N_1 \leq 1$ is generally set first to increase the impact angle to meet the constraint. And then, $N_2 > 2$ is set to ensure trajectory convergence.

2.3. Motivations. In principle, BPNG is similar to VCPNG in terms of the manner of satisfying the impact angle constraints. In both methods, the trajectory is pulled up in the first stage of guidance, so as to create a large impact angle

condition. When the impact angle is equal to the expected impact angle, the constraint is satisfied. Subsequently, PPNG makes the trajectory converge, and the impact point constraint is satisfied. So, the process can be divided into two phases: first stage creates the impact angle condition, while second stage ensures the trajectory convergence.

In existing research, under the condition that there is no real-time LOS distance feedback, the time-to-go is commonly estimated according to the initial LOS distance and velocity. Then, the bias term is evenly distributed to the first stage. Once the integral component is equal to the required bias integral component, the bias term will be cancelled and PPNG in the second phase will begin immediately. So, the control strategy of BPNG is [25]

$$b = \begin{cases} \dfrac{B_N V_0}{R_0} & B < B_N, \\ 0 & B \geq B_N. \end{cases} \tag{14}$$

In VCPNG, $N_1 \leq 1$ is set in the first stage, and $N_2 > 2$ is set in the second stage. The judgment criteria of switching from the first stage to the second stage is as follows: when the proportion coefficient is N_2, the corresponding impact angle calculated by (10) is equal to expected impact angle Γ. Once the condition $\theta_f \leq -\Gamma$ is satisfied, the terminal phase is immediately entered. So, the control strategy of VCPNG is [25]

$$N = \begin{cases} N_1 & \theta_f > -\Gamma, \\ N_2 & \theta_f \leq -\Gamma. \end{cases} \tag{15}$$

Through the aforementioned method, both the impact point constraint and the impact angle constraint can be satisfied under ideal conditions.

However, there are two problems in the above methods.

(1) The guidance command saltation exists at the switching of the guidance phase. In the two-stage proportional guidance methods BPNG and VCPNG proposed in [25], the guidance commend will saltate because of the discontinuous changes of the bias term and proportional coefficient during the guidance phase switching. The drastic saltation of guidance commend will bring great pressure to the control system. In serious cases, the attitude of the aircraft will be unstable or even out of control. In order to solve the problem of guidance command saltation without real-time LOS distance, a SBPNG method based on BPNG method is proposed

(2) According to the previous analysis, in the BPNG and VCPNG methods, the adjustment of the impact angle only exists in the first stage. The second stage is PPNG, which can only satisfy the attack point constraint. So, whether BPNG or VCPNG, the impact angle control is not reflected in the guidance instruction in the second stage. Thus, they belong to open-loop control. Considering the disturbance faced by the aircraft in the course of flight, the accuracy of the impact angle cannot be guaranteed under these methods. Therefore, the UPNG is proposed based on SBPNG to realize the closed-loop control of impact angle without line-of-sight distance

Table 1: Initial parameters.

Parameter	Value	Unit
X-coordinate of the target	2500	m
Y-coordinate of the target	0	m
X-coordinate of the vehicle	0	m
Y-coordinate of the vehicle	150	m
Initial LOS distance	2504	m
Initial flight path angle	0	°
Initial LOS angle	3.4	°
Vehicle velocity	200	m/s
Max bias term (k)	0.35	—
Duration of the bias term (t_N)	13.29	s

3. Smooth-Biased Proportional Navigation Guidance

According to the definition of normal overload, the required normal acceleration can be expressed as follows:

$$a = V\dot{\theta}. \tag{16}$$

According to the open-loop BPNG, the bias term is added to the first stage and removed in the second stage. Thus, the saltation of required normal acceleration occurs during the switch between these two stages. In the current guidance and control process, the guidance system usually generates the corresponding angle of attack (AOA) to the control system according from the required normal acceleration [30].

$$\alpha = \frac{ma}{C_y^\alpha q s_m}, \tag{17}$$

where C_y^α denotes lift coefficient, q denotes dynamic pressure, and s_m denotes aerodynamic area. Saltation of the required acceleration a will result in that of the AOA, which should be avoided as far as possible in the design of guidance and control systems. If there is a saltation, the control system cannot immediately adjust the state to the command value. The response process of control system is a main source of impact angle errors in open-loop control.

The saltation is caused by the sudden introduction and cancellation of the bias term. As shown in (12), the effect of the impact angle control will be the same, as long as the integral component of the bias term B is certain. Therefore, a smoothing method based on the trigonometric function

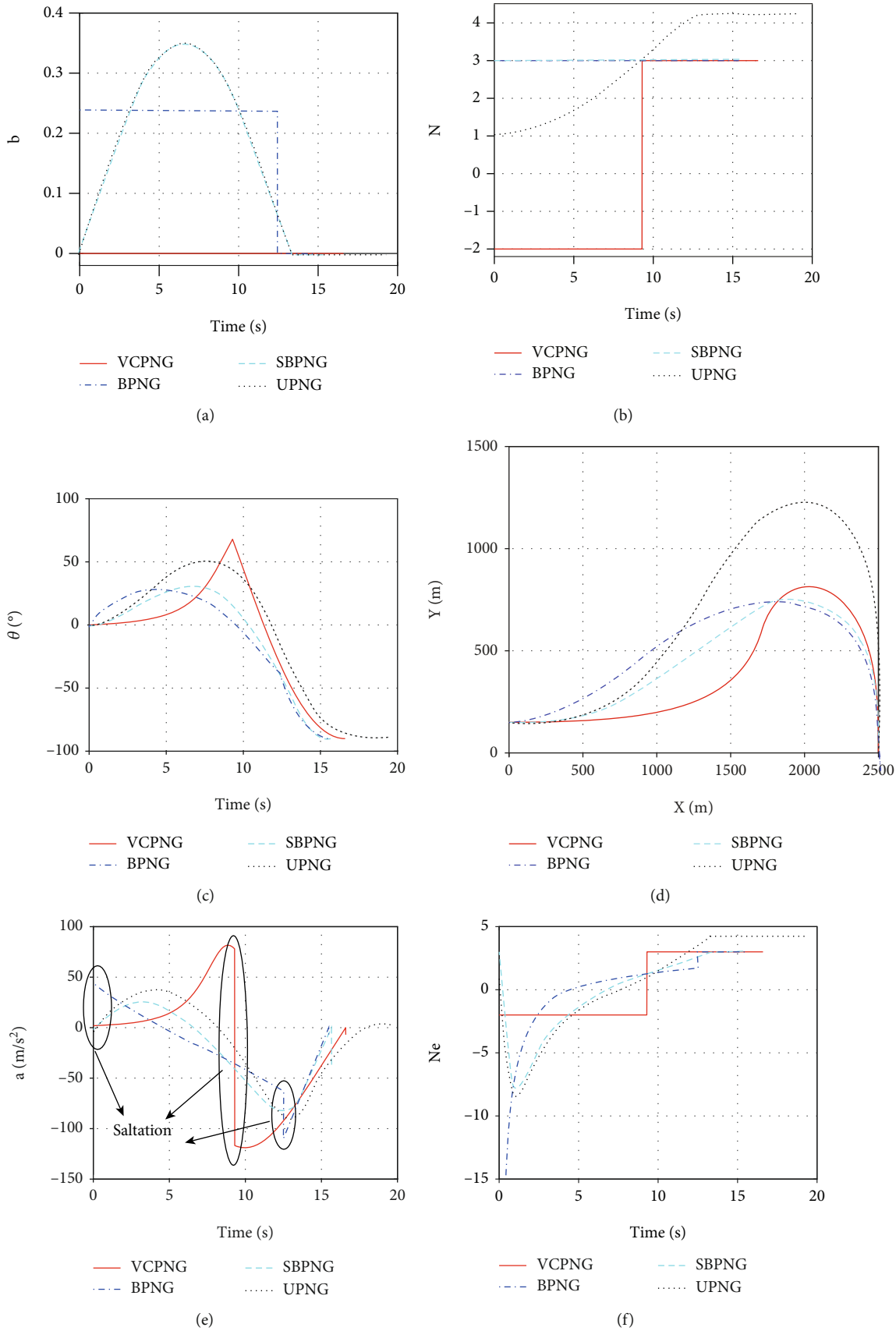

Figure 2: Simulation results of relative motion model for attacking a fixed target. (a) Bias. (b) Proportional coefficient. (c) Flight path angle. (d) Trajectory. (e) Required acceleration. (f) Effective coefficient.

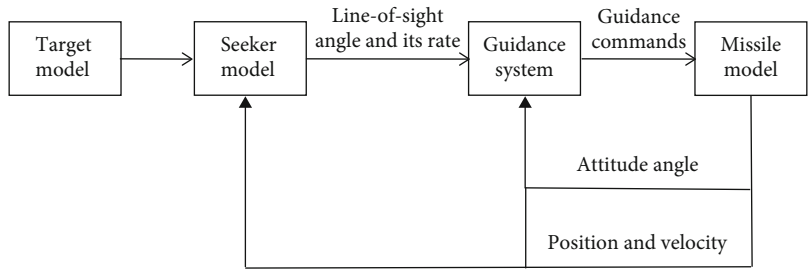

Figure 3: Framework of dynamic model.

Table 2: Vehicle parameters.

Parameter	Value	Unit
Takeoff mass	29.7	kg
Reference length	1.7	m
Reference area	0.02698	m^2
Seeker max ranging distance	1500	m
Max bias term (k)	1.25	—
Duration of the bias term (t_N)	11.42	s

was established in this paper:

$$b = k \sin\left(\frac{t}{t_N}\pi\right), \tag{18}$$

where k is the peak value of the bias term, which can be determined according to the maximum required acceleration that the vehicle can provide and t_N indicates duration of the bias term. The integral component of the bias term is obtained by integrating (18).

$$B = \int_{t_0}^{t_0+t_N} k \sin\left(\frac{t}{t_N}\pi\right) dt = 2\frac{t_N}{\pi}k. \tag{19}$$

According to the previous analysis, once $B = B_N$, the impact angle is equal to the expected impact angle. Hence, from (13) and (19), the expression of t_N can be obtained as

$$t_N = \frac{(N-1)\Gamma + Nq_0 - \theta_0}{2k}\pi. \tag{20}$$

The corresponding control logic can be described as follows:

$$b = \begin{cases} k \sin\left(\dfrac{t}{t_N}\pi\right) & t < t_N, \\ 0 & t > t_N. \end{cases} \tag{21}$$

4. United Proportional Navigation Guidance

Although the SBPNG method can smooth the guidance command, its control of the impact angle still exists only in the first stage. Therefore, like BPNG and VCPNG, it belongs to open-loop control. The UPNG method is proposed to realize the closed-loop control of the impact angle in the whole guidance process under the condition of no real-time LOS distance. Several scholars [15, 29] have studied the VCPNG method with impact angle constraints in closed-loop control, but real-time LOS distance or time-to-go need to be provided. There are few closed-loop control guidance schemes at present without LOS distance or time-to-go. In this paper, combined with the related properties of VCPNG and SBPNG, a closed-loop control method UPNG without LOS distance was established.

According to (1), (2), (3), and (4), the partial derivative of θ, η with respect to R can be easily obtained.

$$\frac{d\theta}{dR} = \frac{N \tan\eta}{R}, \tag{22}$$

$$\frac{d\eta}{dR} = \frac{(N-1)\tan\eta}{R}. \tag{23}$$

Taking N as a constant and integrating (23),

$$\sin\eta = \sin\eta_0 \left(\frac{R}{R_0}\right)^{N-1}. \tag{24}$$

Divide (22) by (23) and substitute (24):

$$d\theta = \frac{N}{N-1}\frac{1}{\sqrt{1-\left(\sin\eta_0 (R/R_0)^{N-1}\right)^2}} d\left(\sin\eta_0\left(\frac{R}{R_0}\right)^{N-1}\right). \tag{25}$$

By integrating (25), the variation law of flight path angle θ with LOS distance R can be obtained as

$$\theta_1 = \frac{N}{N-1}\arcsin\left(\sin\eta_0\left(\frac{R}{R_0}\right)^{N-1}\right)\Bigg|_{R_0}^{R_1} + \theta_0. \tag{26}$$

As a result, the coefficient corresponding to the impact angle constraint in the current state can be deduced:

$$N = \frac{\theta - \theta_f}{q - \theta_f}. \tag{27}$$

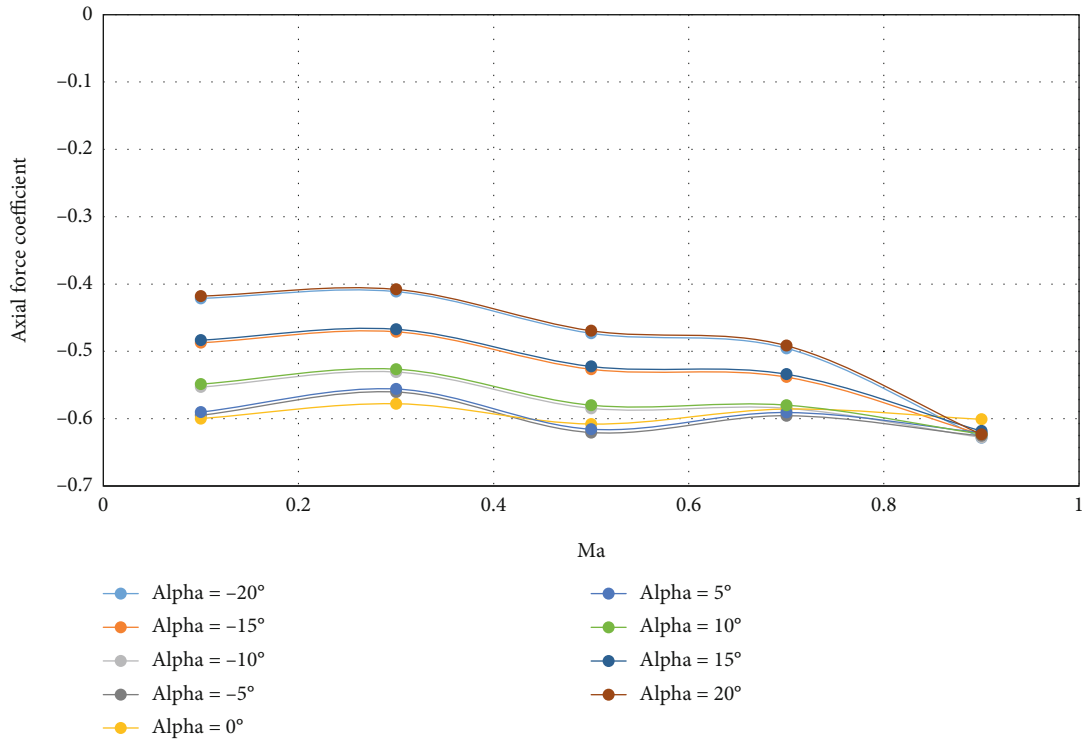

Figure 4: Axial force coefficient.

Taking the derivative of (27) with respect to time,

$$\dot{N} = \frac{\dot{\theta}(q-\theta_f) - \dot{q}(\theta-\theta_f)}{(q-\theta_f)^2}. \tag{28}$$

By substituting (4), (27), and (28), $N' = 0$ can be found. So, the proportional coefficient N will remain unchanged in the whole guidance process without considering external disturbance. For PNG with large impact angle constraints, the initial N calculated by (27) is usually less than 2. According to Section 2.1, if the proportional coefficient N is less than 2, the terminal overload will diverge. So, when the initial N value is less than 2, this method cannot be used alone. In order to ensure the terminal required acceleration convergence, the bias term can be added. In the early phase, due to the effect of the bias term, the impact angle can be increased, and the proportion coefficient will also be increased. When the proportional coefficient N is greater than 2, the bias term can be removed and the second stage will be activated. For the disturbance in the second stage, the variable coefficient can be adjusted adaptively to the closed-loop control with impact angle constraints. The corresponding control strategy is as follows:

$$\dot{\theta} = \frac{\theta-\theta_f}{q-\theta_f}\dot{q} + b. \tag{29}$$

The bias term b is the same as (21). In UPNG method, impact angle is constrained by bias term b and variable coefficient N defined by (27). This not only gets the guidance command continuous and smooth. The closed-loop control of impact angle is also realized under the action of adaptive variable coefficient. To verify the validity and correctness of the method, a large number of numerical simulation results are given as follows.

5. Numerical Simulations

In order to fully verify the guidance performance of the designed guidance laws, a relative motion model and a dynamic model were established. The former model is simple and usually used for the design of the guidance method without considering the variation of the velocity and the force on the vehicle. In the latter model, an experimental aircraft, closing the real flight, is built to test the proposed guidance law. This model includes thrust, gravity, aerodynamics, and other external forces as well as the seeker model. The four methods of VCPNG, BPNG, SBPNG, and UPNG were simulated and compared. SBPNG and UPNG methods were proposed in this paper, and VCPNG and BPNG methods were used for comparative analysis which were proposed in [25]. The constraints of impact angle in the simulation were all set as $\Gamma = 90°$.

5.1. Homing Guidance. The relative motion model was discussed in Section 1. The specific parameters of the trajectory simulation are shown in Table 1. The velocity is assumed to be constant during guidance.

According to the above parameters, VCPNG, BPNG, SBPNG, and UPNG, were simulated, respectively, and the results are shown in the following figures.

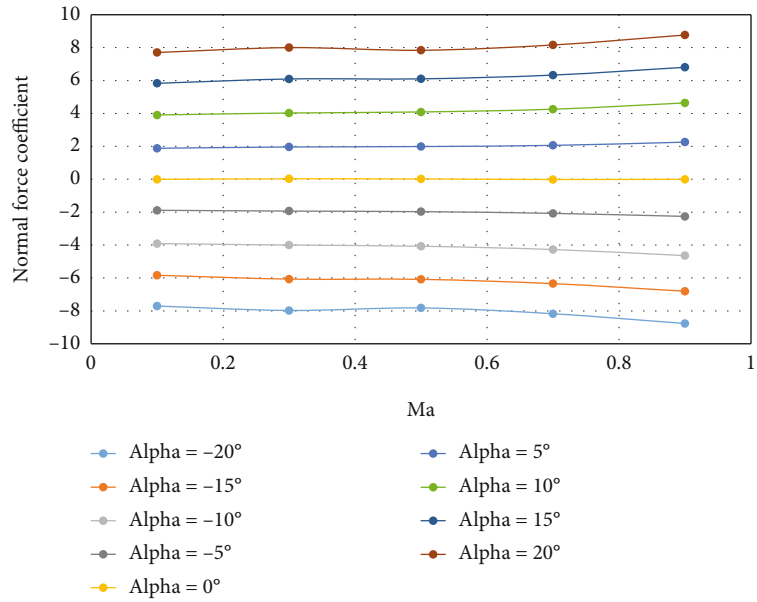

Figure 5: Normal force coefficient.

Table 3: Values of thrust and mass varying with time.

t (s)	0.000	0.246	0.484	0.722	0.96	1.198	1.436	1.675	1.914
T (KN)	1.699	2.412	2.445	2.463	2.471	2.476	2.478	2.475	2.467
m (kg)	29.700	29.480	29.250	29.010	28.760	28.510	28.260	28.010	27.760
t (s)	2.154	2.396	2.651	2.946	3.279	3.654	4.082	4.58	5.179-∞
T (KN)	2.455	2.273	1.572	1.066	0.747	0.508	0.324	0.188	0.000
m (kg)	27.510	27.270	27.050	26.880	26.740	26.630	26.540	26.480	26.430

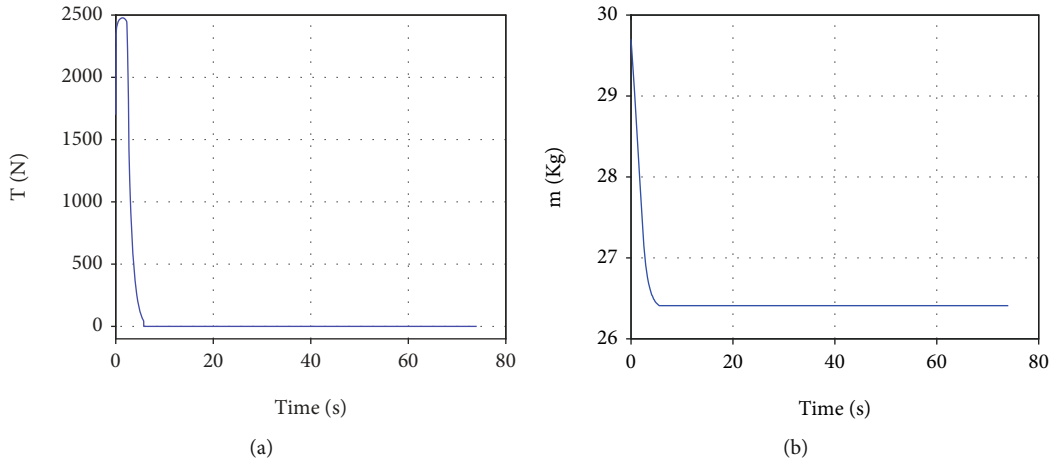

Figure 6: The variation curves of thrust and mass. (a) Thrust. (b) Mass.

As it can be seen from Figures 2(c) and 2(d), the impact angle constraints and impact point constraints of the four methods were satisfied. As shown in Figure 2(a), in order to ensure that the total bias integral value was constant, the maximum bias value of the SBPNG and UPNG was larger than that of the BPNG. Figure 2(e) reveals that in the BPNG and VCPNG methods, saltation of the required acceleration occurred at the beginning and end of the first stage. The required maximum overload of different methods could be arranged in descending order as follows: VCPNG, BPNG,

UPNG, and SBPNG. So, the smooth processing is helpful to reduce the maximum overload. According to the definition of convergence trajectory, the effective proportional coefficient N_e should be greater than 2. There are clear trajectory convergence points for the VCPNG, BPNG, and SBPNG methods. According to Figures 2(a), 3(b), and 2(f), the switching time of the proportional coefficient corresponded to the trajectory convergence point of the VCPNG method. The end time of the bias term corresponded to the trajectory convergence point of the BPNG and SBPNG methods. The UPNG method was affected by both the bias term and the time-varying coefficient so that there was no clear convergence point. Thus, the trajectory would converge adaptively and have a better adaptive effect in the case of external disturbance.

5.2. Dynamic Model for Attacking a Fixed Target. The dynamic model includes the vehicle model and seeker model, which simulate the motion of a vehicle and the measurements of the LOS angle and LOS angle rate. Under the guidance command, the vehicle can accurately hit the target satisfying certain constraints. The framework of the simulation model is shown in Figure 3.

The scenario of the simulation was set as follows: a vehicle was launched toward the target at a distance of 5500 m, at an elevation angle of 65° from the ground. It would arrive near the target according to a designed trajectory, and then, the seeker captured the target and entered the terminal guidance phase. The specific parameters are shown in Table 2.

The dynamic model of the vehicle is based on previous research, and the following assumptions were adopted:

(1) The earth is regarded as a homogeneous sphere, ignoring the influence of the earth's oblateness

(2) The influence of the earth's rotation is ignored, and the atmosphere is stationary relative to the earth and is uniform at the same height

(3) For the coordinate transformation 3-2-1, the Euler rotation order is used

Based on the aforementioned assumptions, a simplified dynamic model in the launch coordinate system was obtained [30].

$$
\begin{aligned}
m\begin{bmatrix}\frac{dv_x}{dt}\\ \frac{dv_y}{dt}\\ \frac{dv_z}{dt}\end{bmatrix} &= G_B\begin{bmatrix}T+X\\ Y\\ Z\end{bmatrix} + m\frac{g}{r}\begin{bmatrix}x\\ y+R_e\\ z\end{bmatrix},\\
G_B &= \begin{bmatrix}\cos\varphi\cos\psi & \cos\varphi\sin\psi\sin\gamma-\sin\varphi\cos\gamma & \cos\varphi\sin\psi\cos\gamma+\sin\varphi\sin\gamma\\ \sin\varphi\cos\psi & \sin\varphi\sin\psi\sin\gamma+\cos\varphi\cos\gamma & \sin\varphi\sin\psi\cos\gamma-\cos\varphi\sin\gamma\\ -\sin\psi & \cos\psi\sin\gamma & \cos\psi\cos\gamma\end{bmatrix},\\
\begin{bmatrix}\frac{dx}{dt}\\ \frac{dy}{dt}\\ \frac{dz}{dt}\end{bmatrix} &= \begin{bmatrix}v_x\\ v_y\\ v_z\end{bmatrix},\\
\begin{bmatrix}X\\ Y\\ Z\end{bmatrix} &= \begin{bmatrix}C_{x1}qS\\ C_{y1}qS\\ C_{z1}qS\end{bmatrix},\\
\theta &= \arctan\frac{v_y}{v_x},\\
\sigma &= -\arcsin\frac{v_z}{V},\\
m &= m_0 - \dot{m}t,\\
\sin\psi &= \sin\sigma\cos\alpha\cos\beta-\sin\alpha\cos\sigma\sin\nu+\cos\alpha\sin\beta\cos\sigma\cos\nu,\\
\sin\varphi\cos\psi &= \cos\alpha\cos\beta\sin\theta\cos\sigma+\sin\alpha(\sin\theta\sin\sigma\sin\nu+\cos\theta\cos\nu)-\cos\alpha\sin\beta(\sin\theta\sin\sigma\cos\nu-\cos\theta\sin\nu),\\
\sin\gamma\cos\psi &= \sin\alpha\cos\beta\sin\sigma+\cos\alpha\cos\sigma\sin\nu+\sin\alpha\sin\beta\cos\sigma\cos\nu.
\end{aligned}
\tag{30}
$$

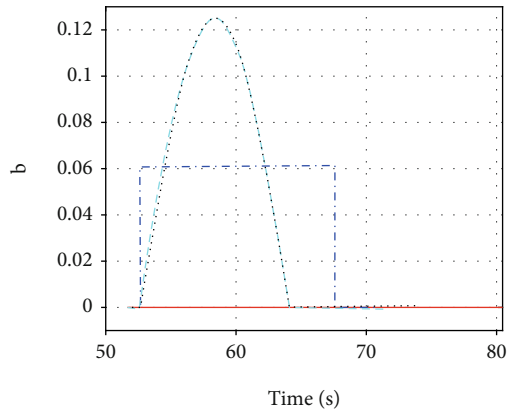

(a)

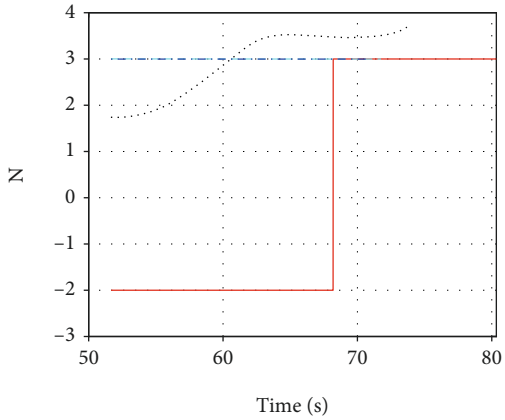

(b)

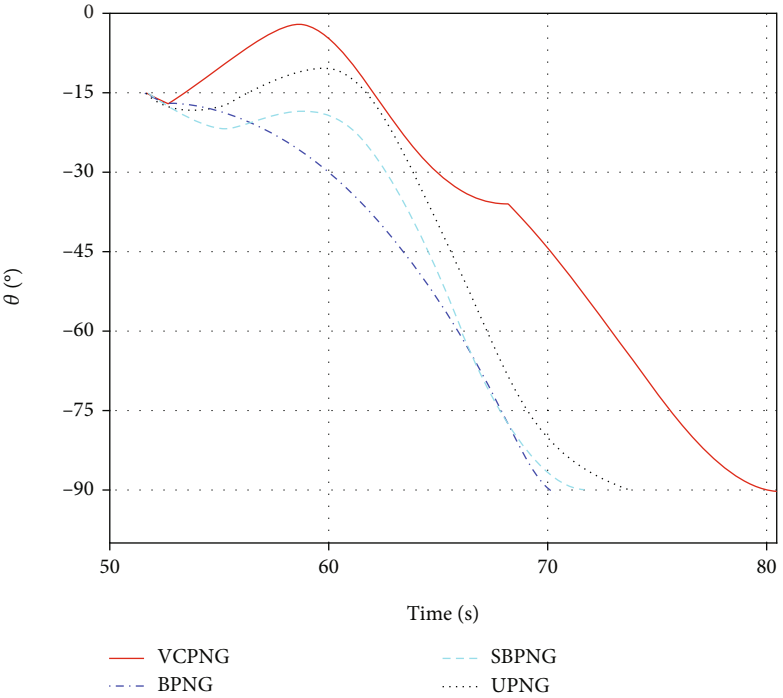

(c)

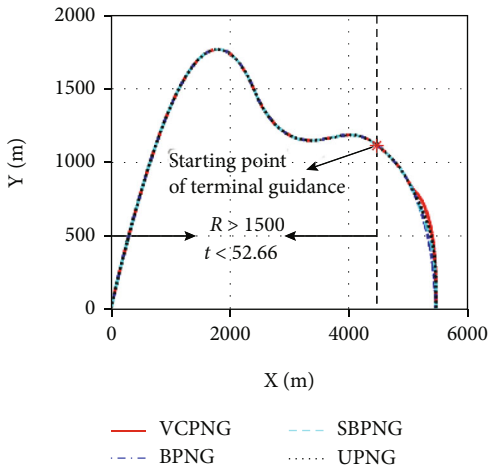

(d)

Figure 7: Continued.

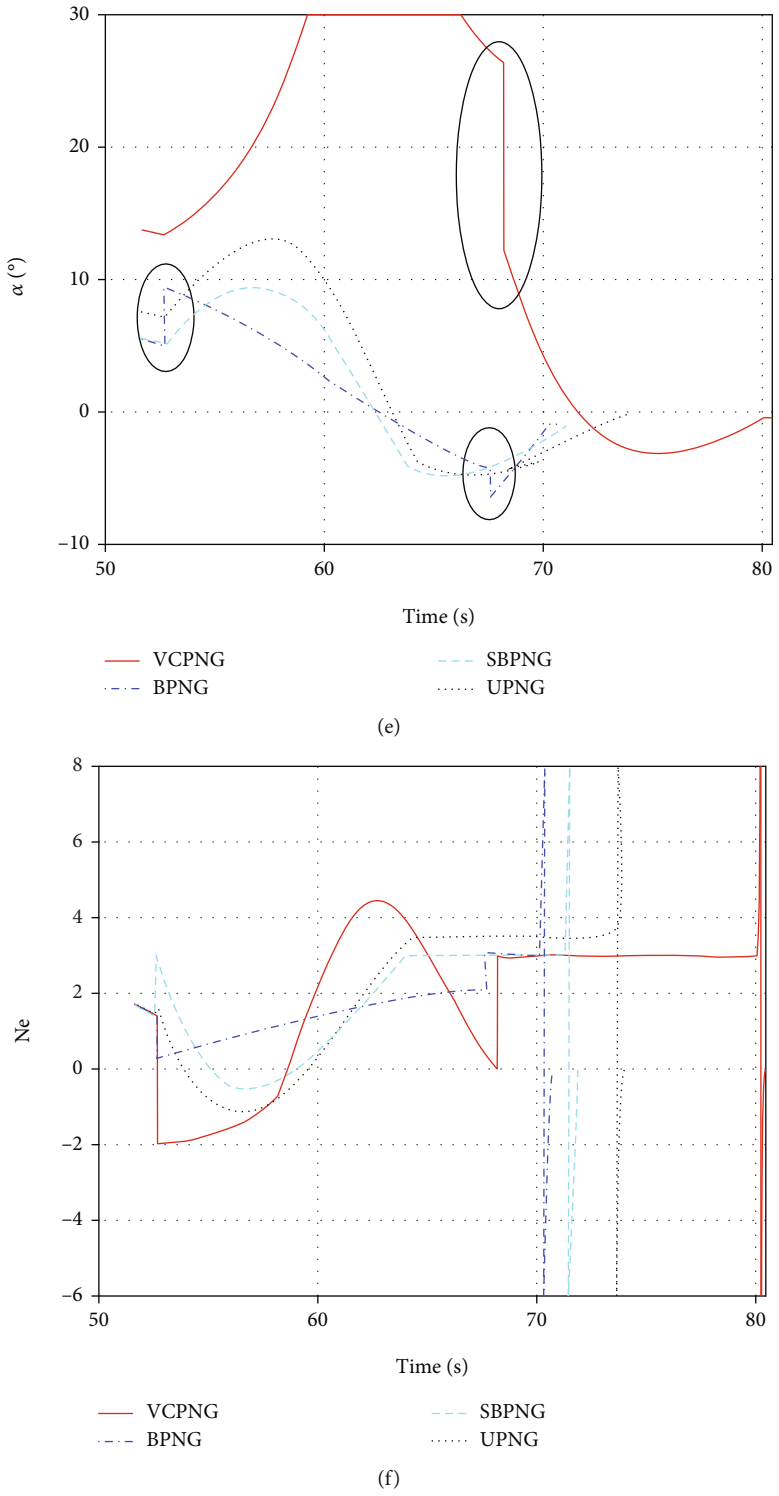

Figure 7: Simulation results of the dynamic model for attacking a fixed target. (a) Bias. (b) Proportional coefficient. (c) Flight path angle. (d) Trajectory. (e) Bias command AOA. (f) Effective coefficient.

In the model, the aerodynamic coefficients C_{x1}, C_{y1}, and C_{z1} are functions of AOA, sideslip angle, and Mach number. The specific relationships are shown in Figures 4 and 5. In the simulation, the motion in the longitudinal plane was mainly considered. Since the design of the lateral motion remained 0, the lateral force coefficient C_{z1} was 0.

The values of thrust and mass during flight are shown in Table 3.

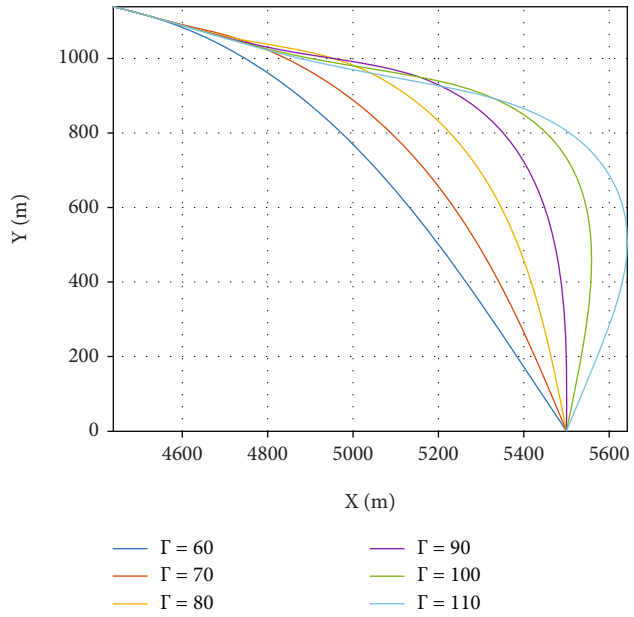

(a)

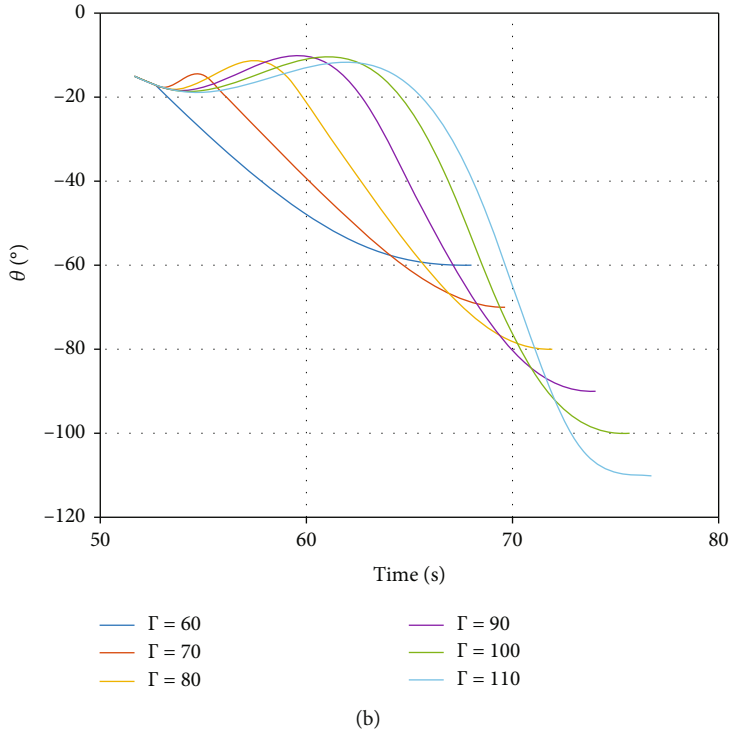

(b)

Figure 8: Continued.

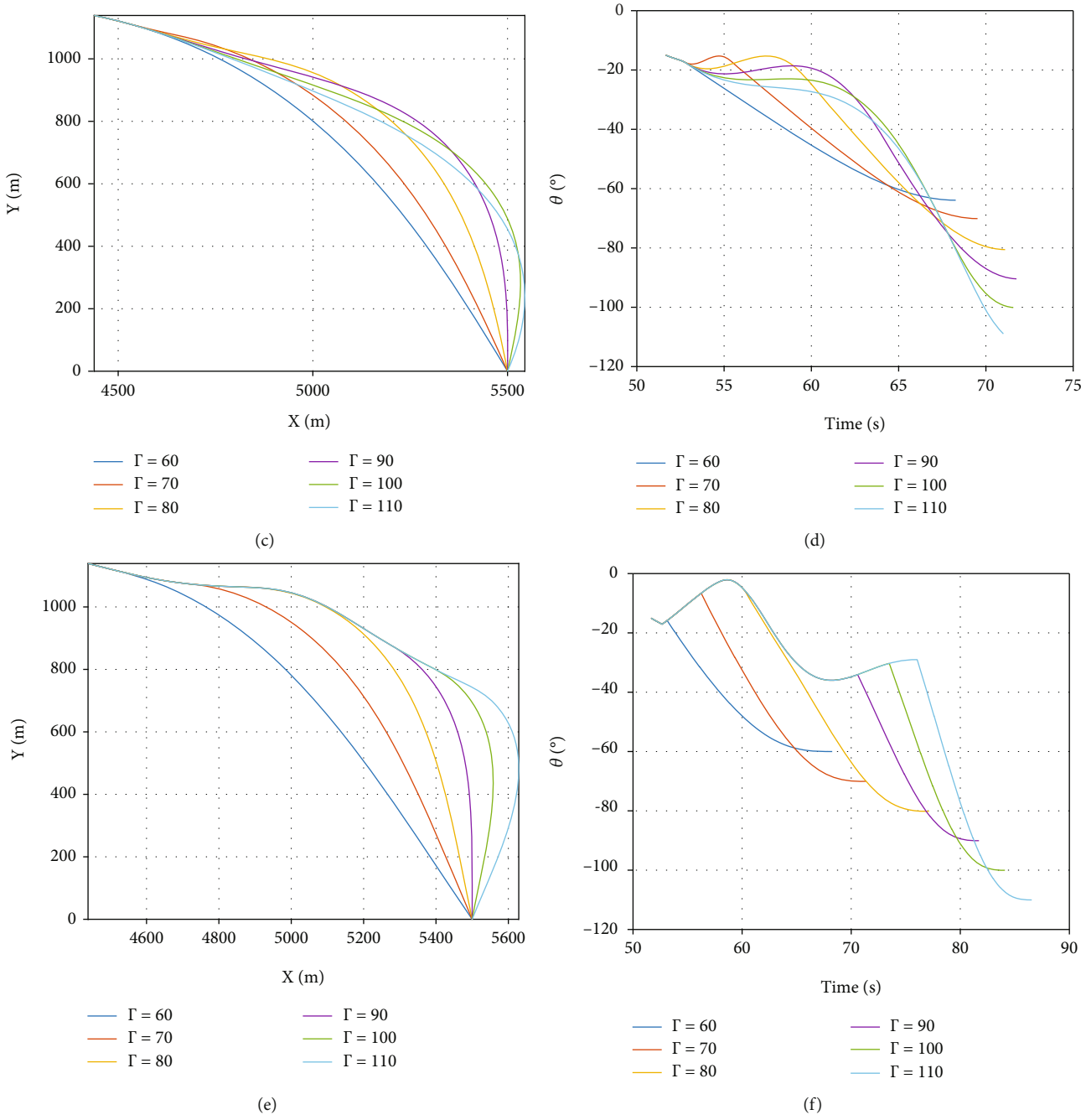

Figure 8: Continued.

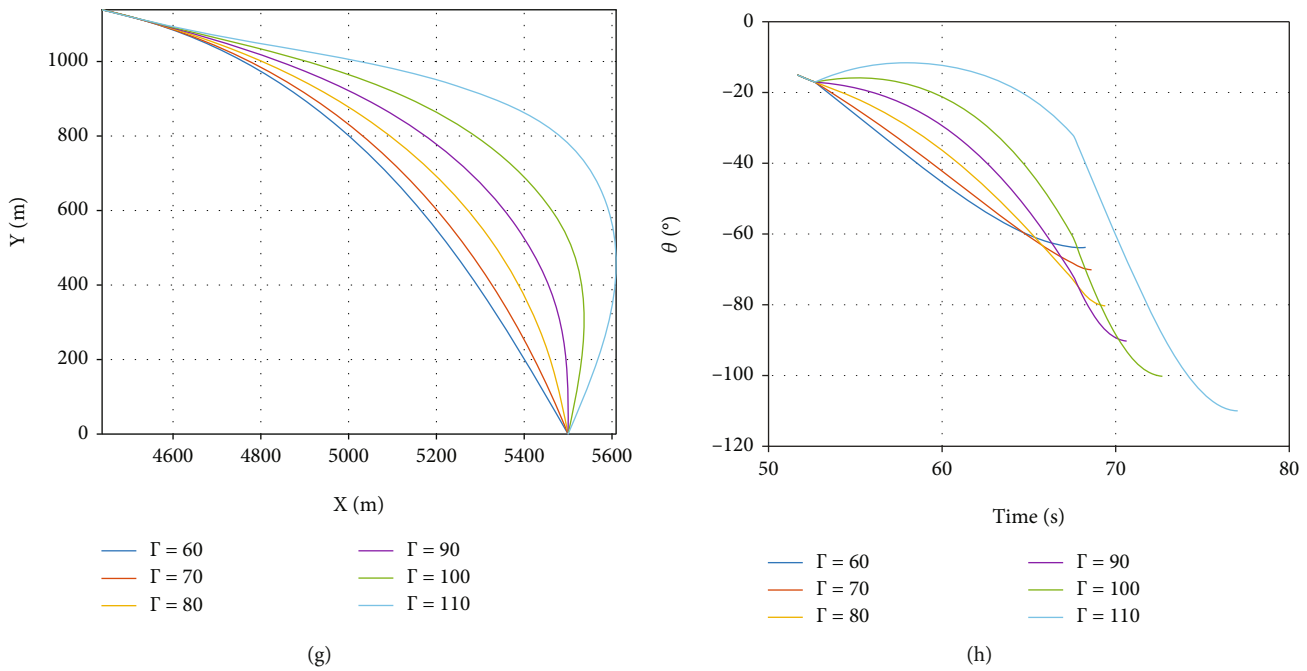

Figure 8: The results of simulation experiments under different expected impact angles. (a) Trajectory under the UPNG method. (b) Flight path angle under the UPNG method. (c) Trajectory under the SBPNG method. (d) Flight path angle under the SBPNG method. (e) Trajectory under the VPNG method. (f) Flight path angle under the BPNG method. (g) Trajectory under the BPNG method. (h) Flight path angle under the BPNG method.

Table 4: Errors of impact point and impact angle under different expected impact angles.

Error	Method	60°	70°	80°	90°	100°	110°
Impact point (m)	UPNG	0.3642	0.2962	-0.0475	-0.0025	-0.0575	-0.1970
	SBPNG	0.2919	-0.0517	0.0297	-0.0090	-0.0799	-0.1026
	VPNG	0.2919	-0.0843	-0.0192	-0.0078	-0.0039	0.0900
	BPNG	0.2844	0.0574	-0.0719	-0.0206	-0.0328	-0.2748
Impact angle (°)	UPNG	0.0035	-0.0161	-0.0128	-0.0132	-0.0116	-0.1546
	SBPNG	-3.9066	-0.1052	-0.5613	-0.4249	-0.0976	1.0425
	VPNG	-3.9066	-0.0776	-0.2387	-0.1779	-0.1194	-0.1204
	BPNG	-3.7790	-0.1337	-0.3305	-0.2816	-0.2326	-0.0017

Table 5: The disturbance parameters and their ranges.

Number	Deflection parameter	Error distribution form	Deflection range (%, 3σ)
1	Mass deflection	Normal distribution	[-0.015,0.015]
2	Thrust deflection	Normal distribution	[-0.05,0.05]
3	Density deflection	Normal distribution	[-0.1,0.1]
4	Axial aerodynamic deflection	Normal distribution	[-0.15,0.15]
5	Normal aerodynamic deflection	Normal distribution	[-0.1,0.1]
6	Wind speed	Uniform distribution	[-5,5] m/s

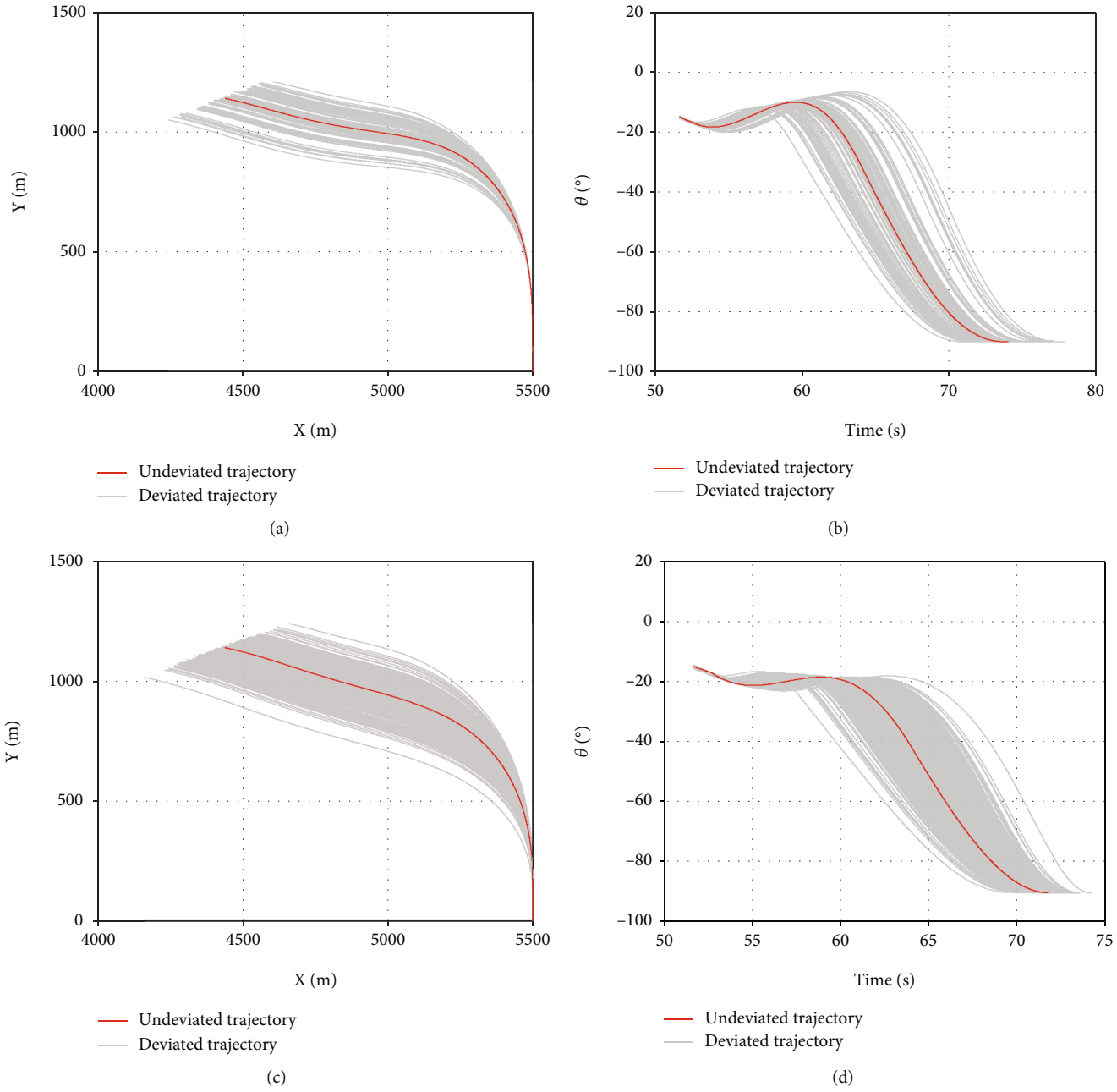

Figure 9: Continued.

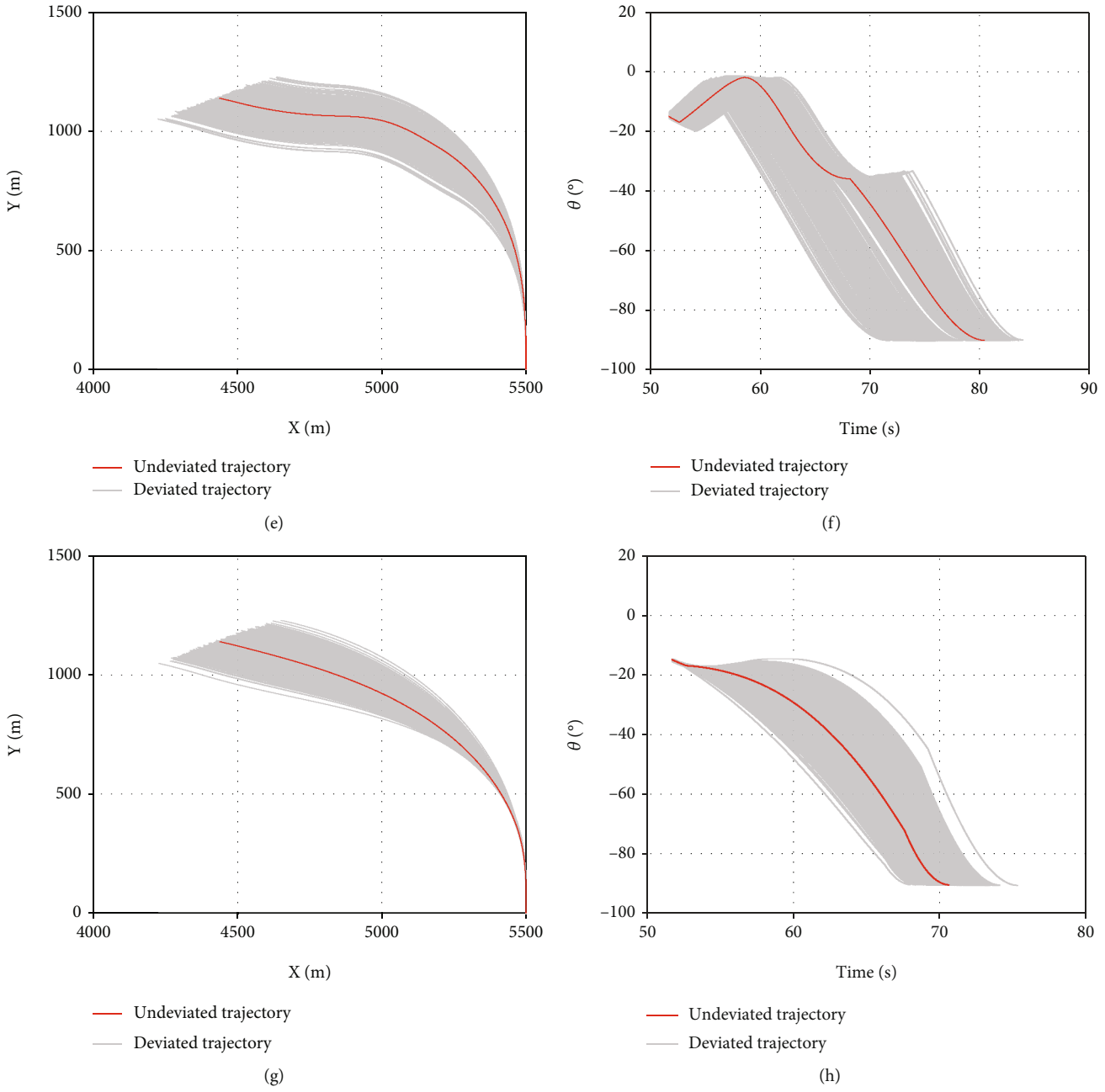

Figure 9: The results of Monte Carlo simulation experiment. (a) Trajectory under the UPNG method. (b) Flight path angle under the UPNG method. (c) Trajectory under the SBPNG method. (d) Flight path angle under the SBPNG method. (e) Trajectory under the VPNG method. (f) Flight path angle under the VPNG method. (g) Trajectory under the BPNG method. (h) Flight path angle under the BPNG method.

Figure 6 shows the curve of thrust and mass.

Guidance information is provided by the seeker model.

$$\vec{R} = \begin{bmatrix} X \\ Y \\ Z \end{bmatrix} = \begin{bmatrix} X_T - X_M \\ Y_T - Y_M \\ Z_T - Z_M \end{bmatrix}, \tag{31}$$

$$\vec{V} = \begin{bmatrix} V_x \\ V_y \\ V_z \end{bmatrix} = \begin{bmatrix} V_{Tx} - V_{Mx} \\ V_{Ty} - V_{My} \\ V_{Tz} - V_{Mz} \end{bmatrix}, \tag{32}$$

$$\begin{cases} R = \sqrt{X^2 + Y^2 + Z^2} \\ V = \sqrt{V_x^2 + V_y^2 + V_z^2} \end{cases}, \tag{33}$$

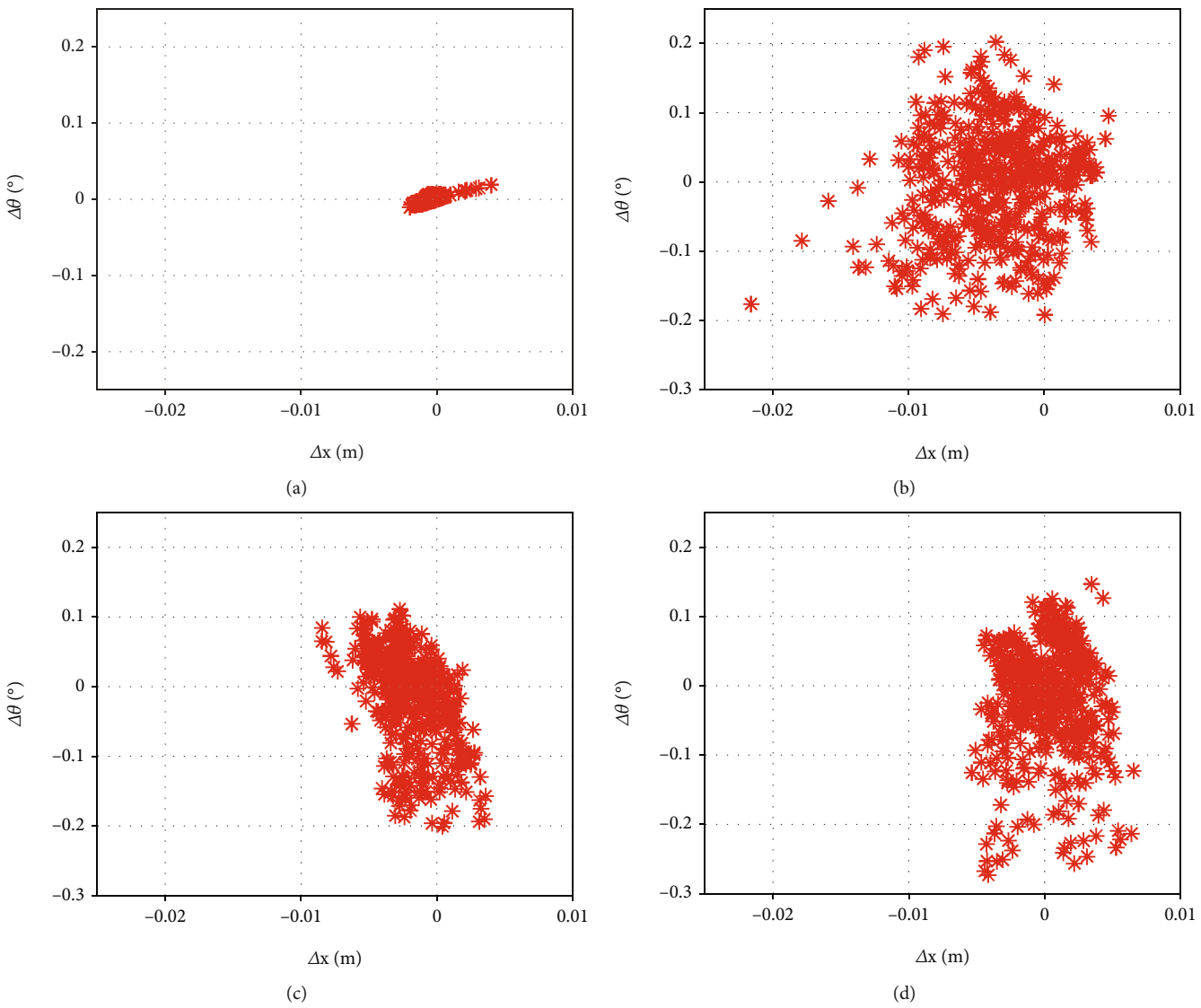

Figure 10: Error distribution of Monte Carlo simulation experiment. (a) UPNG. (b) SBPNG. (c) VPNG. (d) BPNG.

where R and V denote the relative position and velocity vectors of the vehicle and the target, respectively.

$$q_1 = \arctan\left(\frac{Y}{\sqrt{X^2 + Z^2}}\right), \tag{34}$$

$$q_2 = \arctan\left(\frac{-Z}{X}\right), \tag{35}$$

$$\dot{q}_1 = \frac{\left(X^2 + Z^2\right)V_y - Y\left(XV_x + ZV_z\right)}{R^2\sqrt{X^2 + Z^2}}, \tag{36}$$

$$\dot{q}_2 = \frac{V_x Z - XV_z}{X^2 + Z^2}. \tag{37}$$

q_1 and q_2 denote the elevation and azimuth of the LOS angle, respectively, and $\dot{q}_1$ and $\dot{q}_2$ denote their rates. The simulation mainly considered the motion in the longitudinal plane, and thus, the lateral motion parameters were set to 0.

Figure 7 shows the numerical simulation results.

As can be seen from Figure 7(d), the start time of the terminal guidance is 52.66 s. The rest of the figures only show the curves of the terminal guidance stage.

The simulation results verified the feasibility of the proposed method. It can be seen from Figures 7(c) and 7(d) that the constraints of impact angle and impact point were all satisfied in the four methods. An observation can be made from Figure 7(e) that through smooth processing, the command AOA of the SBPNG and the UPNG changed continuously without saltation, while saltation occurred occurs in VCPNG and BPNG. There was divergence in the end effective coefficients of all the four methods, as shown in Figure 7(f). Such divergence could be attributed to the LOS distance being too small and the LOS angle rate changing sharply when the vehicle approached the target. The simulation results show that the phenomenon would occur when

the LOS distance was less than 30 m. In order to prevent such phenomenon in engineering applications, the guidance command remains unchanged when the LOS distance is less than a certain threshold which will not cause a large deviation.

To verify the stability of the guidance method, simulation experiments under different expected impact angles Γ are conducted. The following experiments are carried out under the same guidance starting point. The scheme is aimed at the attack missions with large impact angle. Therefore, considering the limited maneuverability of the vehicle, the expected impact angle is set in the range of 60°-110°. The results are as follows:

Meanwhile, the corresponding errors of impact point and impact angle are listed as follows:

According to Figure 8 and Table 4, UPNG and SBPNG proposed by this paper, and VPNG and BPNG as comparisons, all show a good stability under different expected impact angle constraints. However, the UPNG method has a smaller impact angle error than the other three methods and shows conspicuous advantages especially under the condition of $\Gamma = 60°$. Based on the above results, it can be inferred that both guidance methods proposed in this paper show a good stability under different impact angle constraints. The UPNG method outperforms other methods in impact angle constraints, owing to its closed-loop control method in impact angle.

5.3. Monte Carlo Simulation Experiment. The above simulation experiments are conducted under ideal conditions without considering external disturbance. However, in practical flight, the uncertainty disturbance resulted from complex environment will increase the pressure of guidance system. To verify the robustness of the designed guidance law in the face of various uncertainties, 500 Monte Carlo simulation experiments were carried out under the four guidance laws. The constraints of impact angle in the simulation were all set as $\Gamma = 90°$. The disturbance parameters and their ranges are designed as Table 5.

The simulation results are as follows:

It can be seen from Figure 9 that the initial position of guidance varies substantially when considering all kinds of disturbance. Since the vehicle follows the designed pitch angle sequence before guidance, the changes in the initial flight path angle remain insignificant. The results show that all four methods can satisfy the impact point and impact angle constraints with a certain precision. For further observation, the error distribution map of impact point and impact angle is shown as follows under the same coordinate scale:

The above errors are obtained by the difference between the simulation results and the design values. In the figures, the y-axis represents the impact angle error, and the x-axis denotes the impact point error. Comparing the subgraphs in Figure 10, it can be readily inferred that the impact angle error of UPNG method proposed in this paper is one order of magnitude smaller than that of the other three methods. Meanwhile, it has a relatively small impact point error when considering various external uncertainties. The UPNG method performs better than the other three methods because its closed-loop control method has stronger robustness.

6. Conclusions

In this paper, with the aim of overcoming the guidance command saltation caused by the PNG method without LOS distance, the SBPNG method based on the trigonometric function was proposed. The initial LOS distance information is no longer required to estimate the total guidance time, and the maximum overload of the vehicle was used to design the bias term instead. The simulation results show that SBPNG method could effectively overcome the command saltation. Based on SBPNG method, the UPNG method, combining SBPNG method and VCPNG method was proposed. Under the UPNG method, the bias integral component, bias duration, and proportional coefficient switching time do not need to be strictly controlled anymore. Because of the continuous existence of impact angle control in the whole guidance process by adjusting the proportional coefficient in UPNG method, the closed-loop control of impact angle is realized. The stationary target attack simulation experiment and Monte Carlo simulation experiment were carried out. For hitting the stationary target on the ground, the simulation results show that the four guidance methods could meet the constraints of impact point and impact angle. Compared with the BPNG and VCPNG methods, the SBPNG and UPNG methods proposed in this study could effectively solve the problem of guidance command saltation. For the Monte Carlo simulation experiment, the simulation results show that the UPNG method has stronger robustness in impact angle control.

Nomenclature

$R, \dot{R}$: LOS distance and its rate
$q, \dot{q}$: LOS angle and its rate
$\theta, \dot{\theta}$: Flight path angle and its rate
$\eta, \dot{\eta}$: Look-ahead angle and its rate
N: Proportional guidance coefficient
θ_0, θ_f: Initial and terminal flight path angle
q_0, q_f: Initial and terminal LOS angle
b: Bias term
B_N: Required bias integral component
t_N: Duration of the bias term
N_1, N_2: Proportional guidance coefficient of first stage and second stage
Γ: Expected impact angle.

Data Availability

The program code data used to support the findings of this study are available from the corresponding author upon request.

Conflicts of Interest

The authors declare that there is no conflict of interest regarding the publication of this paper.

Acknowledgments

This work is supported by the National Natural Science Foundation of China under the research grant of U21B2028.

References

[1] M. Kim and Y. Kim, "Lyapunov-based pursuit guidance law with impact angle constraint," *IFAC Proceedings Volumes*, vol. 47, no. 3, pp. 2509–2514, 2014.

[2] M. W. Fossier, "The development of radar homing missiles," *Journal of Guidance, Control, and Dynamics*, vol. 7, no. 6, pp. 641–651, 1984.

[3] X. Hu, S. Yang, and F. Xiong, "Stability of spinning missile with homing proportional guidance law," *Aerospace and Electronic Systems*, vol. 71, pp. 546–555, 2017.

[4] G. Franzini, L. Tardioli, L. Pollini, and M. Innocenti, "Visibility augmented proportional navigation guidance," *Journal of Guidance, Control, and Dynamics*, vol. 41, no. 4, pp. 987–995, 2018.

[5] Z. Jiang, J. Ge, Q. T. Xu, and T. Yang, "Impact time control cooperative guidance law design based on modified proportional navigation," *Aerospace*, vol. 8, no. 8, p. 231, 2021.

[6] K. B. Li, L. Chen, and X. Z. Bai, "Differential geometric modeling of guidance problem for interceptors," *Science China Technological Sciences*, vol. 54, no. 9, pp. 2283–2295, 2011.

[7] Y. Zhao, X. Liao, X. S. Chi, and X. L. Song, "A survey of terminal constrained guidance law," *Aerospace Control*, vol. 35, no. 2, pp. 89–98, 2017.

[8] S. Sun, H. Zhang, and D. Zhou, "A survey of terminal guidance law," *Aerospace Control*, vol. 30, no. 1, pp. 86–96, 2012.

[9] B. S. Kim, J. G. Lee, and H. S. Han, "Biased PNG law for impact with angular constraint," *IEEE Transactions on Aerospace and Electronic Systems*, vol. 34, no. 1, pp. 277–288, 1998.

[10] Y. Zhang, G. Ma, and H. Wu, "A biased proportional navigation guidance law with large impact angle constraint and the time-to-go estimation," *Proceedings of the Institution of Mechanical Engineers, Part G: Journal of Aerospace Engineering*, vol. 228, no. 10, pp. 1725–1734, 2014.

[11] S. Brainin and R. McGhee, "Optimal biased proportional navigation," *IEEE Transactions on Automatic Control*, vol. 13, no. 4, pp. 440–442, 1968.

[12] Z. An, F. F. Xiong, and Z. N. Liang, "Landing-phase guidance of rocket using bias proportional guidance and convex optimization," *Acta Aeronautica et Astronautica Sinica*, vol. 41, no. 5, pp. 247–260, 2020.

[13] S. Lee, S. Ann, S. Cho, and Y. Kim, "Capturability of guidance laws for interception of nonmaneuvering target with field-of-view limit," *Journal of Guidance, Control, and Dynamics*, vol. 42, no. 4, pp. 869–884, 2019.

[14] H. Zhang, S. Tang, J. Guo, and W. Zhang, "A two-phased guidance law for impact angle control with seeker's field-of-view limit," *International Journal of Aerospace Engineering*, vol. 2018, Article ID 7403639, 13 pages, 2018.

[15] H. G. Kim, J. Y. Lee, H. J. Kim, H. H. Kwon, and J. S. Park, "Look-angle-shaping guidance law for impact angle and time control with field-of-view constraint," *IEEE Transactions on Aerospace and Electronic Systems*, vol. 56, no. 2, pp. 1602–1612, 2020.

[16] H. Cho, C. Ryoo, A. Tsourdos, and B. White, "Optimal impact angle control guidance law based on linearization about collision triangle," *Journal of Guidance, Control, and Dynamics*, vol. 37, no. 3, pp. 958–964, 2014.

[17] G. P. Bong, H. K. Tae, and J. T. Min, "Optimal impact angle control guidance law considering the seeker's field-of-view limits," *Proceedings of Institution of Mechanical Engineers Part G Journal of Aerospace Engineering*, vol. 227, no. 8, pp. 1347–1364, 2013.

[18] K. S. Erer and M. K. Ozgoren, "Control of impact angle using biased proportional navigation," in *AIAA Guidance, Navigation, and Control (GNC) Conference*, Boston, MA, 2013.

[19] K. Erer and O. Merttopçuoglu, "Indirect control of impact angle against stationary targets using biased PPN," in *AIAA Guidance, Navigation, and Control Conference*, Toronto, Ontario, Canada, 2010.

[20] K. S. Erer and O. Merttopçuoglu, "Indirect impact-angle-control against stationary targets using biased pure proportional navigation," *Journal of Guidance, Control, and Dynamics*, vol. 35, no. 2, pp. 700–704, 2012.

[21] G. Sun, Q. Wen, X. U. Zhiqiang, and Q. Xia, "Impact time control using biased proportional navigation for missiles with varying velocity," *Chinese Journal of Aeronautics*, vol. 33, no. 3, pp. 956–964, 2020.

[22] A. Ratnoo, "Analysis of two-stage proportional navigation with heading constraints," *Journal of Guidance, Control, and Dynamics*, vol. 39, no. 1, pp. 156–164, 2016.

[23] R. Tekin and K. S. Erer, "Switched-gain guidance for impact angle control under physical constraints," *Journal of Guidance, Control, and Dynamics*, vol. 38, no. 2, pp. 205–216, 2015.

[24] A. Ratnoo and D. Ghose, "Impact angle constrained guidance against nonstationary nonmaneuvering targets," *Journal of Guidance, Control, and Dynamics*, vol. 33, no. 1, pp. 269–275, 2010.

[25] G. S. Wang, *Research on Precision Guidance Technology for Guided Ammunition*, Beijing Institute of Technology, Beijing, China, 2016.

[26] A. Ratnoo, "Analysis of two-stage proportional navigation with impact angle and field -of -view constraints," in *AIAA Guidance, Navigation, and Control Conference*, Florida, 2015.

[27] S. Zhou, S. Zhang, and D. Wang, "Impact angle control guidance law with seeker's field-of-view constraint based on logarithm barrier Lyapunov function," *IEEE Access*, vol. 8, pp. 68268–68279, 2020.

[28] K. Amit, K. S. Nikhil, and H. Sikha, "Impact angle constrained time-optimal guidance law for stationary target interception in 3D," in *AIAA SCITECH 2022 Forum*, San Diego, CA & Virtual, 2022.

[29] P. Lu and B. David, "Adaptive terminal guidance for hypervelocity impact in specified direction," *Journal of Guidance, Control, and Dynamics*, vol. 29, no. 2, pp. 269–278, 2006.

[30] K. Chen, L. Liu, and H. Meng, *Launch Vehicle Flight Dynamics and Guidance*, National Defense Industry Press, Beijing, China, 2014.